Embedded systems as programmable square wave generator in wireless power transfer

Sabriansyah Rizqika Akbar, Eko Setiawan, Achmad Basuki
Department of Informatics Engineering, Faculty of Computer Science, Universitas Brawijaya, Malang, Indonesia

Article Info

ABSTRACT

This study focuses on the design and development of programmable frequency generator using embedded devices that are able to produce square wave signals in the wireless power transfer (WPT) transmitter. We validate the accuracy of the output signal by measuring distance error. We validate that our system can change and sweep the frequency and produce high power by measuring the absorbed power in the load. We conduct the frequency sweep analysis to find optimal frequency and the frequency splitting phenomenon. The experiments show that the system can produce and sweep the square wave signals with less than 1% error. We also find that the frequency splitting occurred when distance among two coils in the range 0.5-6.5 cm and the splitting disappeared when the distance is above 7.5 cm. The frequency splitting shows that the measured optimum frequency differs from the calculation. The difference confirms that the programmable frequency generator is needed to adjust the frequency that can transfer maximum power to the load.
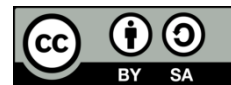
Corresponding Author:

Sabriansyah Rizqika Akbar
Department of Informatics Engineering, Faculty of Computer Science, Universitas Brawijaya
Veteran Street, Ketawanggede, Lowokwaru, Malang City, East Java, Indonesia
Email: sabrian@ub.ac.id

1. INTRODUCTION

Tesla [1] famous patent entitled "Apparatus for transmitting electrical energy" has been inspired many researchers in delivering wireless power transfer (WPT) system into reality today. We can now deliver energy without physical wires using the physics phenomenon of energy conversion into electricity. WPT (from the distance between transmitter and receiver point-of-view) can be classified into far-field and near-field WPT. The far-field WPT systems are built using laser and microwave. The laser WPT considers light source as the WPT transmitter by converting electrical energy to a laser beam [2]. Currently, the laser based WPT is studied to be applied in several fields such as terrestrial and space applications, internet of things, and aircraft [3], [4]. Another far-field WPT is the microwave WPT. Microwave WPT uses high frequency power radiation from high power oscillators (MHz and GHz). In some research, the microwave WPT can reach hundreds of meters to kilo meter distance in several applications such as satellites, drones, and mobile facilities [5]. The far-field WPT, both of laser and microwave, is considered as radiative WPT technology [6].

On the other hand, near-field WPT is considered a non-radiative WPT technology. The near-field WPT can be developed using fundamental capacitive [7] or inductive [8] circuit. The capacitive WPT uses pairs of metal plates coated with the dielectric materials that produce electric fields between the transmitter and receivers [9]. Another near-field WPT category is the inductive WPT. The inductive WPT principle is based on faradays laws. As current flows through the primary coils, it generates a magnetic flux, leading to

electromagnetic induction in the secondary coils and subsequently causing current to flow in the secondary circuits. The current flow in the secondary circuit is influenced by the mutual inductance between coils [8]. Currently, inductive WPT has gained more popularity, as it is utilized in mobile device charger technology and has become standardized [10]. Other than mobile devices, inductive WPT research began to expand the have been used in many applications such as unmanned aerial vehicle (UAV) [11]–[13] or biomedical implants [14]. The inductive WPT system can be constructed using electronic circuits, consisting of both primary and secondary circuits. The primary and secondary circuit is compensated with additional components (such as capacitor) since researchers want to obtain the maximum power absorbed by the load receivers in the secondary circuit. The compensation networks consist of series-series, series-parallel, parallel-series, and parallel-parallel circuits. Each of the compensation networks have several pros and cons depending on the WPT system requirements [15].

In the current study, the maximum WPT powers can be obtained using calculation theories. The most generic theory is by calculating the resonant frequency. Alternatively, we can obtain the mathematical models of the WPT circuit [16] and then conduct the optimization using partial derivatives on some parameters [17] or use the heuristic algorithm such as genetic algorithms or particle swarm optimizations (PSO) [18]. Afterwards, we can apply the frequency response or calculate the average power to validate the calculations. By finding the optimum frequency point we can gain maximum power absorbed by the receivers. Even though we can obtain the maximum power theoretically, there exists mutual inductance parameter in the calculation that will be difficult to estimate since it depends on the coupling coefficient between -1 to 1. The coupling coefficient depends on the quality of the copper (or materials), distance, and angle of the primary and secondary coils. Using measured distance between coils, we can determine the optimum frequency of WPT system [19], [20]. The system requires additional distance sensor and the placement of the sensor must be precise.

An additional challenge in the WPT can occur in real-world situations such as frequency splitting phenomenon. The frequency splitting phenomenon happens when the distance between coils is bigger than the critical value and the peak from the frequency points will change to double peak. This situation makes the optimum frequency point is shifted from the calculation [21]–[24]. Therefore, the need to sweep the frequency (at some range) in the WPT devices must be conducted.

This study will focus on the design and development of programmable square wave function generator for WPT system using generic and common embedded devices. Our system will be able to deliver programmable functionality in the frequency generator so it will be able to select the frequency on demand. We validate our system by measuring the output power absorbed by the load. Since we are using square wave signal, the harmonics of the sine wave will create a phenomenon in the frequency response that shows the optimum points will have set of patterns of the local and the global peak.

2. METHOD

In order to gain high power WPT circuit need to be compensated. The compensation means topology and components used to bring the high power WPT. WPT circuit can be compensated using series-series, series-parallel, parallel-series, or parallel-parallel. In this study, we choose the series-parallel compensation circuit since we are using it for low-power applications and lower dc link voltage. In this situation the series-parallel circuit is better than others compensation circuit [25]. Our proposed circuit is described in Figure 1. The basic WPT primary circuit consists of AC voltage source $u(t)$, internal resistance of voltage source R_s, the capacitor C_1 and the coil L_1 as primary coil with the resistance R_1. The current flow in the coil will generate electromagnetic inductions to L_2 affected with mutual inductance $M = K\sqrt{L_1 L_2}$, where K is the coupling coefficient between -1 and 1 that can be represented with distance or misalignment between primary and secondary coils [26], [27]. The secondary circuit consists of the L_2 coil with R_2 as the resistance. Since we are using series-parallel compensation circuit we put the capacitor C_2 in parallel with the L_2 coil for the secondary circuit.

We conduct the simulations using the software simulation program with integrated circuit (LTSPICE). The circuit parameter configuration is used as in Table 1. Further, we simulate the circuit using frequency response (1 V AC voltage) sweep between 100 Hz to 130 kHz for 250 points. The result is plotted using Python matplotlib as in Figure 2. The inductance of WPT circuit consists of primary inductance and secondary inductance where each inductance comes from copper coils. We use the series-parallel configuration and match the frequency resonant formula $f = 1/(2\pi\sqrt{LC})$ and calculate the optimum frequency point is located at 53.14 kHz.
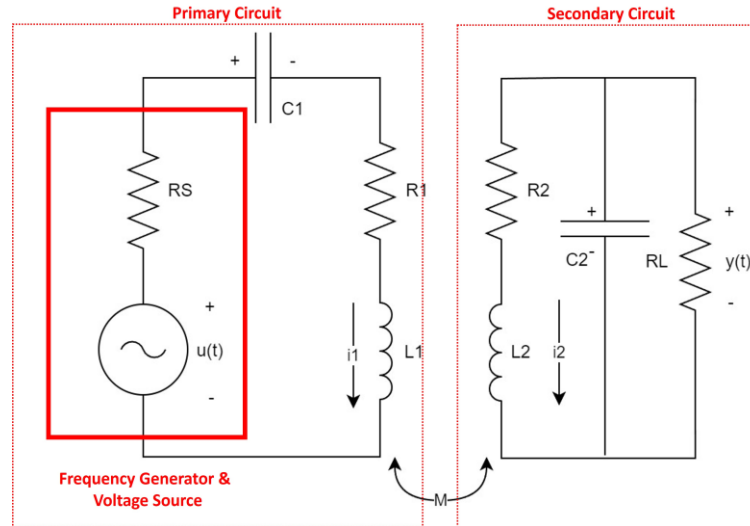
Figure 1. WPT system with series parallel circuit

Table 1. WPT configuration for primary and secondary circuit

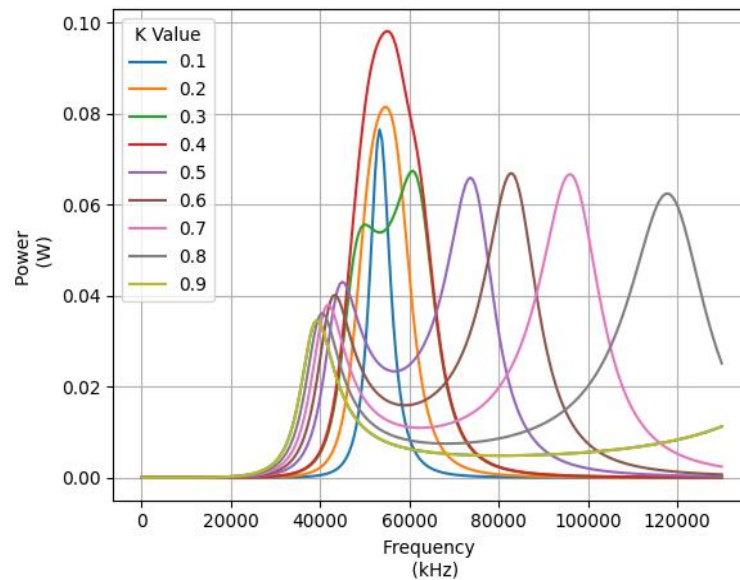| Parameters	Value
Thickens	1 mm
Diameter coils	8 cm
Winding	20 Turns
Coil length	8 cm
Coil inductance	89.7 µH
Capacitors (C_1 & C_2)	100 nF
Load resistor	100 Ω

Figure 2. Simulation results

From Figure 2, we see that the optimal frequency is not always in one point. When the K value is above 0.2, the frequency splitting happens, and the optimum frequency points are split into two. Since we saw that the optimum frequency is moving during the K value changes, we still need to change the frequency and find the highest point that produces the highest power. Therefore, we propose the architecture of a programmable square wave function generator as shown in Figure 3 to perform frequency sweep and find the

proper working frequency that transfers the highest power. The architecture consists of the microcontroller, the H-bridge and the WPT transmitter circuit. The microcontroller produces a programmable pulse width modulation (PWM) output based on the frequency demands. The output PWM voltage from microcontrollers is amplified by the H-bridge to produce higher peak-to-peak voltage that can be used to drive the WPT transmitter circuit. Figure 4 demonstrates the PWM output voltage produced by microcontrollers (0 to 5 V) amplified by the H-bridge (-8 V to +8 V).
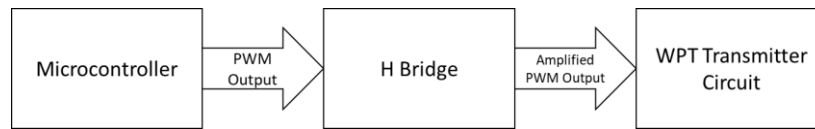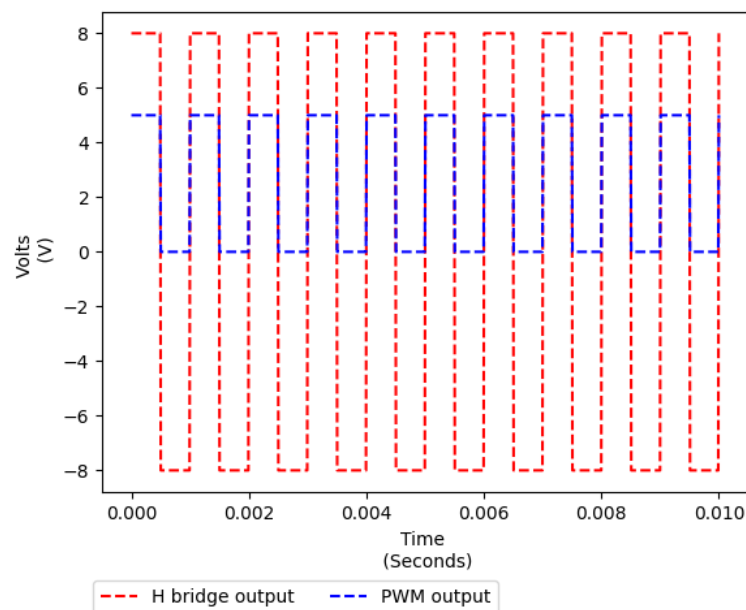
Figure 3. Generic proposed architecture

Figure 4. PWM output and H-bridge output

Our proposed functional requirements for square wave function generator consists of three states which are set frequency, increase frequency, and decrease frequency. The set frequency is the default state where the system will hold the value of frequency. Our function generator can increase or decrease when the users press the increase/decrease frequency button. Afterwards, the generator will increase or decrease its frequency for 1 kHz and hold the frequency for the current frequency +/- 1 kHz and display the hold frequency in the organic light-emitting diode (OLED).

The proposed function generator circuit is shown in Figure 5. The generator utilize embedded system Raspberry Pi Pico [28] as microcontrollers and uses the IRF3205 based H-bridge modules as amplifier. The Pico GPIO 18 serves as the PWM pin. We also provide two push-button switches to increase or decrease the frequency value. The GPIO 18 pin is connected to the H-bridge direction pin, while the PWM input (PWM1 and PWM2 in the H-bridge) configured to be always high. The PWM duty cycle was set on 50%. The MTR1+ pin and MTR1- pin are connected to WPT circuit to bring the alternate current voltage. The PWM output will bring the square wave 0 to 5 V. The H-bridge output from the MTR1+ pin and MTR1- pin will bring the square wave voltage output peak-to-peak ($V_{(p-p)}$) from -8 V to 8 V (Figure 4). To capture the output power at secondary side, we add current, voltage and power monitor (INA219) [29] connected to the Pico using inter-integrated circuit (I2C) interface. Our system implementation can be seen in the Figure 6 where the system consists of raspberry Pico as microcontrollers, buttons and H-bridge IRF3205 modules. The red and green button is equipped to increase and decrease the frequency.
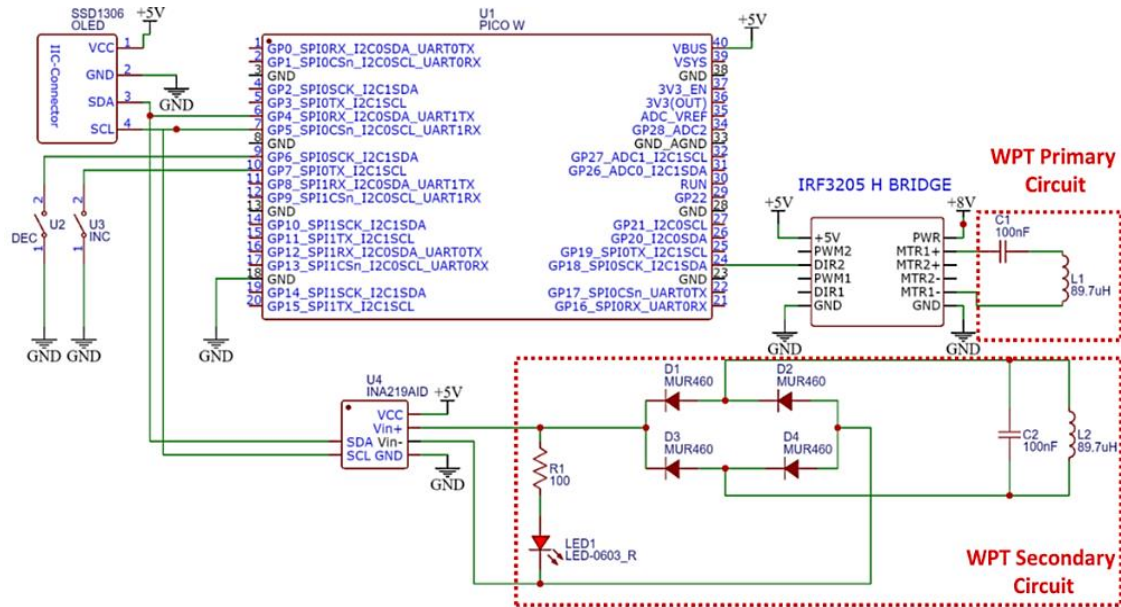
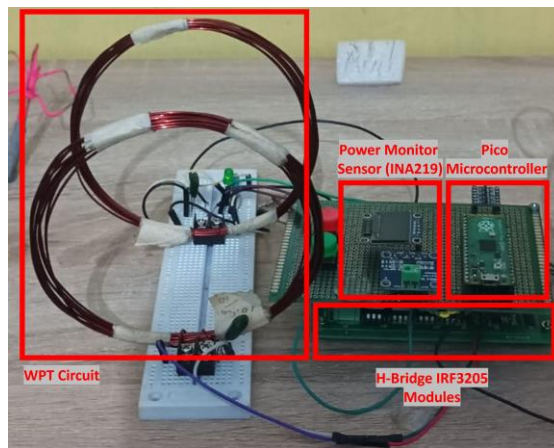Figure 5. Square wave function generator circuit

Figure 6. Programmable square wave function generator for the WPT system

3.   RESULTS AND DISCUSSION

In this section, the study explores the results of our proposed system and analyzes the accuracy of the square wave frequency generator and optimum frequency analysis. The accuracy of frequency generator is discussed in first subsection and the analysis of optimum frequency is briefly discussed in second subsection. Additional details are provided in the following subsections.

3.1. Square wave frequency accuracy

The frequency is swept from 0-130 kHz with a 1 kHz increment. In this experiment, we checked the accuracy of the square wave frequency obtained from the output PWM of Pico microcontrollers and the output frequency after being amplified by the H-bridge. We use oscilloscope to monitor the frequency from the Pico and the H-bridge. Afterwards, we use the distance error calculation to measure the difference between the desired frequency and the frequency output results from the Pico and the H-bridge. The distance error calculation is plotted in Figure 7.

From Figure 7, we see that the distance error for Pico PWM output as well as H-bridge square wave output are less than 1%. This means that the system output, which is the PWM output and the H-bridge, has a good performance regarding the accuracy of the generated desired frequency. This information ensures that we can conduct further analysis for describe the behaviour of power output.
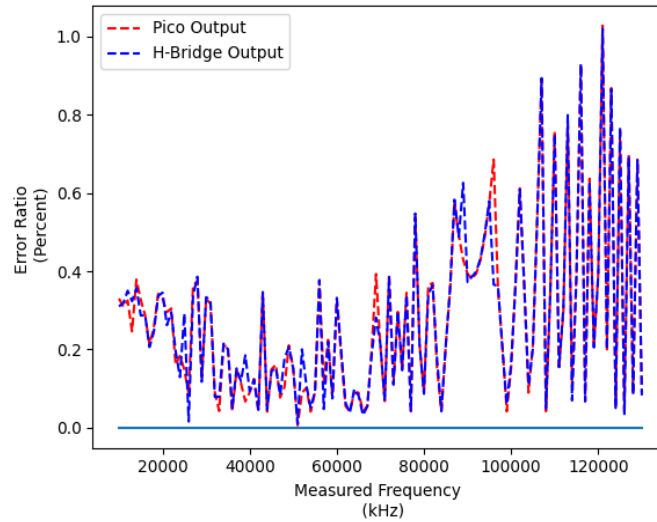
Figure 7. Distance error calculation

3.2. Optimum frequency and harmonic analysis

The peak frequency and harmonic analysis experiment is conducted to find out the maximum power obtained from the WPT circuit load at some frequency point. The maximum power was observed using a frequency sweep from 0 to 130 kHz. The generator uses a square wave signal with configurable frequency value. The square wave signal is composed from the sine-wave signal and the harmonic of the fundamental frequency as in (1) (where L is the square wave period).

$$f(x) = \frac{4}{\pi} \sum_{n=1,3,5,\dots}^{\infty} \frac{1}{n} \sin\left(\frac{n\pi x}{L}\right) \tag{1}$$

Therefore, it will result to create some form of peak consist of local and global peak from the frequency response analysis. Let P is a set of peaks and p^* is the optimal frequency to obtain the maximum power. The output of the swept frequency will create a pattern as in (2) [30].

$$P = \left\{ p^*, \frac{1}{3}p^*, \frac{1}{5}p^*, \frac{1}{7}p^*, \frac{1}{9}p^*, \dots, \frac{1}{2n+1}p^* \right\} \tag{2}$$

Using the power sensor INA219, we measured the actual power absorbed by the 100 Ω load resistor by sweeping frequency across 10 kHz to 130 kHz. We conducted the frequency sweeping and conduct the power monitoring for each distance between 0 to 22 cm. We plot the measurement result in Figures 8 and 9. The results of power monitoring in frequency sweep have locals and global peak.

Figure 8 shows the importance of programmable frequency generator in WPT system. As by design, we already set the resonant frequency to 53.14 kHz. The real-world experiment shows a frequency splitting phenomenon that creates the optimum frequency does not locate exactly at the configured resonant frequency. In the distance of 0.5 cm the optimum frequency is located at 46 kHz. While in the distance of 6.5 cm, the optimum frequency shifted to 54 kHz. Therefore, by using our programmable frequency generator we can adjust the working frequency even though it is not located at the resonant frequency. Figure 8 shows that the optimum frequency p^* has the local peak 1/3 p^*. As an example, we see that in the distance of 6.5 cm, the system detects the p^*=54 kHz. At this distance, the local peak 1/3 p^* was also detected at 18 kHz.

Figure 9 shows the result experiment of power while frequency sweeping. Figure 9(a) shows the power absorbed by load resistor in the distance 7.5 cm to 13.5 cm. The frequency splitting phenomenon does not happen during this range of distance. However, the optimal frequency is located at 55 kHz and not exactly in the 53.14 kHz frequency calculation. In this distance of measurement, we also found that the p^*=55 kHz also having set of local peaks consists of 1/3 p^*=18 kHz and 1/5 p^*=11 kHz.

Figure 9(b) shows the power measurement in 15.5 cm to 21.5 cm. The experiment distance is stopped at 21.5 cm because the WPT does not deliver enough power to turn on the LED on the secondary circuit. Therefore, in the distance measurement experiment shows that the maximum distance able to reach is 21.5 cm with 60.73 mW. The maximum power able to be absorbed by the load is 1293 mW in the 0.5 cm distance.
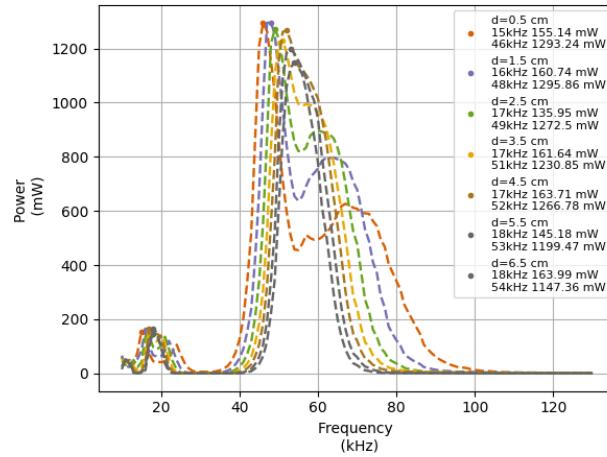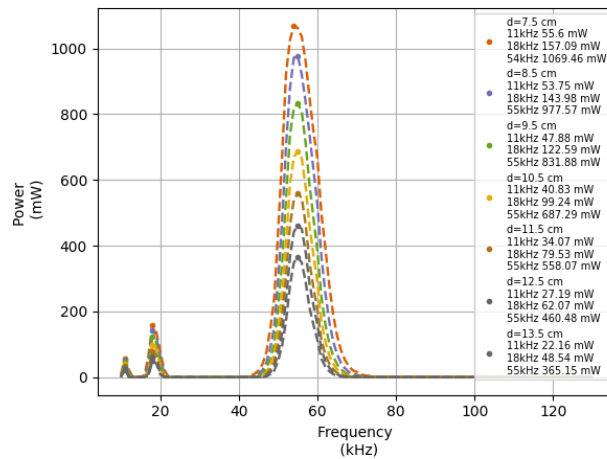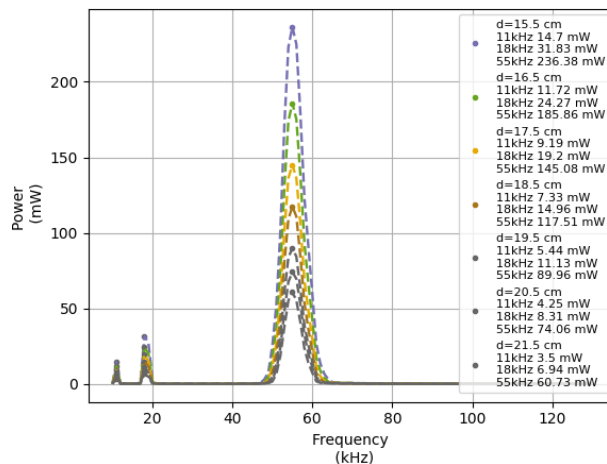
Figure 8. Frequency response results from experiment at 0.5 to 6.5 cm distances

(a)

(b)

Figure 9. Results of frequency response experiment on distance: (a) 7.5 to 13.5 cm and (b) 15.5 to 21.5 cm

4.   CONCLUSION

This study focuses on the development of variable frequency generators using generic embedded devices in the WPT systems. The development of the variable frequency generator starts with the microcontroller's selections based on the PWM features obtained from the microcontroller datasheet.

Afterwards, the PWM output from microcontrollers needs to be increased using amplifiers. The amplifiers can be selected from generic H-bridge modules that are chosen based on the supported voltage and the maximum frequency. This study selects the Pico microcontrollers and the IRF3205 H-bridge modules since we choose the low range frequency below 100 kHz. We use the power sensor (INA219) to monitor power absorbed by the load resistor.

The results of the experiment show that our programmable frequency generator system can be amplified at 8 V (from 5 V) and has frequency accuracy below 1%. From the peak and harmonic analysis, we able to shows that our systems can capture the optimum power along with the local peak pattern. Our systems can reach the 21.5 cm maximum distance (60.73 mW) and the maximum power 1.3 W in 0.5 cm distance. This study also finds that even though we are able to calculate the resonance frequency in the designing phase, the possibilities of the mismatch optimum frequency can be found caused by the frequency splitting phenomenon. Thus, the optimum frequency that produces the high power in WPT systems will be able to be found by using our programmable systems.

In the current circuit we use the power monitor on the secondary sides of the WPT systems. In the future, this study will continue to find methods regarding how to monitor the power absorbed from the load resistors from the primary circuits. This can be conducted by finding correlations between the power measurements comparison (from the primary or secondary circuits) and the distance between coils.

ACKNOWLEDGEMENTS

REFERENCES

[1]   N. Tesla, "Apparatus for transmitting electrical energy," US1119732A, 1907
[2]   S. A. H. Mohsan, H. Qian, and H. Amjad, "A comprehensive review of optical wireless power transfer technology," *Frontiers of Information Technology & Electronic Engineering*, vol. 24, no. 6, pp. 767–800, Jun. 2023, doi: 10.1631/FITEE.2100443.
[3]   K. Jin and W. Zhou, "Wireless laser power transmission: a review of recent progress," *IEEE Transactions on Power Electronics*, vol. 34, no. 4, pp. 3842–3859, Apr. 2019, doi: 10.1109/TPEL.2018.2853156.
[4]   Q. Zhang, W. Fang, Q. Liu, J. Wu, P. Xia, and L. Yang, "Distributed laser charging: a wireless power transfer approach," *IEEE Internet of Things Journal*, vol. 5, no. 5, pp. 3853–3864, Oct. 2018, doi: 10.1109/JIOT.2018.2851070.
[5]   X. Zhu, K. Jin, Q. Hui, W. Gong, and D. Mao, "Long-range wireless microwave power transmission: a review of recent progress," *IEEE Journal of Emerging and Selected Topics in Power Electronics*, vol. 9, no. 4, pp. 4932–4946, Aug. 2021, doi: 10.1109/JESTPE.2020.3038166.
[6]   K. Detka and K. Górecki, "Wireless power transfer—a review," *Energies*, vol. 15, no. 19, p. 7236, Oct. 2022, doi: 10.3390/en15197236.
[7]   C. Lecluyse, B. Minnaert, and M. Kleemann, "A review of the current state of technology of capacitive wireless power transfer," *Energies*, vol. 14, no. 18, p. 5862, Sep. 2021, doi: 10.3390/en14185862.
[8]   Z. Zhang, H. Pang, A. Georgiadis, and C. Cecati, "Wireless power transfer—an overview," *IEEE Transactions on Industrial Electronics*, vol. 66, no. 2, pp. 1044–1058, Feb. 2019, doi: 10.1109/TIE.2018.2835378.
[9]   D. Rozario, N. A. Azeez, and S. S. Williamson, "Comprehensive review and comparative analysis of compensation networks for capacitive power transfer systems," in *2016 IEEE 25th International Symposium on Industrial Electronics (ISIE)*, IEEE, Jun. 2016, pp. 823–829. doi: 10.1109/ISIE.2016.7744996.
[10]   Wireless Power Consortium, "Qi specification: introduction version 1.3." 2021, Accessed: Jan 25, 2024 [Online]. Available: https://www.wirelesspowerconsortium.com/knowledge-base/specifications/download-the-qi-specifications/.
[11]   X. Mou, D. Gladwin, J. Jiang, K. Li, and Z. Yang, "Near-field wireless power transfer technology for unmanned aerial vehicles: a systematical review," *IEEE Journal of Emerging and Selected Topics in Industrial Electronics*, vol. 4, no. 1, pp. 147–158, Jan. 2023, doi: 10.1109/JESTIE.2022.3213138.
[12]   S. Obayashi, Y. Kanekiyo, and T. Shijo, "UAV/drone fast wireless charging FRP frustum port for 85-kHz 50-V 10-A inductive power transfer," in *2020 IEEE Wireless Power Transfer Conference (WPTC)*, IEEE, Nov. 2020, pp. 219–222. doi: 10.1109/WPTC48563.2020.9295562.
[13]   S. Chen, J. Xiao, Q. Chen, X. Wu, and W. Gong, "Research on magnetic integration coupling mechanism of uav wireless power transfer system," in *2021 IEEE 16th Conference on Industrial Electronics and Applications (ICIEA)*, IEEE, Aug. 2021, pp. 1007–1010. doi: 10.1109/ICIEA51954.2021.9516415.
[14]   A. I. Mahmood, S. K. Gharghan, M. A. Eldosoky, and A. M. Soliman, "Near-field wireless power transfer used in biomedical implants: A comprehensive review," *IET Power Electronics*, vol. 15, no. 16, pp. 1936–1955, Dec. 2022, doi: 10.1049/pel2.12351.
[15]   W. Zhang and C. C. Mi, "Compensation topologies of high-power wireless power transfer systems," *IEEE Transactions on Vehicular Technology*, vol. 65, no. 6, pp. 4768–4778, Jun. 2016, doi: 10.1109/TVT.2015.2454292.
[16]   S. Akbar, E. Setiawan, T. Hirata, K. Yamaguchi, and I. Hodaka, "The frequency response and steady-state analysis on wireless power transfer using square wave input," in *6th International Conference on Sustainable Information Engineering and Technology 2021*, New York, NY, USA: ACM, Sep. 2021, pp. 38–43. doi: 10.1145/3479645.3479659.
[17]   S. R. Akbar, E. Setiawan, T. Hirata, and I. Hodaka, "Optimal wireless power transfer circuit without a capacitor on the secondary side," *Energies*, vol. 16, no. 6, p. 2922, Mar. 2023, doi: 10.3390/en16062922.
[18]   S. R. Akbar and I. Hodaka, "A design approach to wireless high-power transfer to multiple receivers with asymmetric circuit," *International Journal of Circuits, Systems and Signal Processing*, vol. 15, pp. 125–134, Feb. 2021, doi: 10.46300/9106.2021.15.14.

[19]   K. Yamaguchi, R. Okamura, H. Terada, and K. Iida, "Experimental review of an improving system on wireless power transfer via auto tuning of frequency," *International Journal of Electrical and Computer Engineering (IJECE)*, vol. 13, no. 2, pp. 1314–1319, Apr. 2023, doi: 10.11591/ijece.v13i2.pp1314-1319.

[20]   K. Yamaguchi, R. Okamura, A. W. Yian Kiat, and K. Iida, "Efficient wireless power transfer for a moving electric vehicle by digital control of frequency," *International Journal of Electrical and Computer Engineering (IJECE)*, vol. 14, no. 2, pp. 1308–1313, Apr. 2024, doi: 10.11591/ijece.v14i2.pp1308-1313.

[21]   X. Liu, X. Yuan, C. Xia, and X. Wu, "Analysis and utilization of the frequency splitting phenomenon in wireless power transfer systems," *IEEE Transactions on Power Electronics*, vol. 36, no. 4, pp. 3840–3851, Apr. 2021, doi: 10.1109/TPEL.2020.3025480.

[22]   Y. Zhang and Z. Zhao, "Frequency splitting analysis of two-coil resonant wireless power transfer," *IEEE Antennas and Wireless Propagation Letters*, vol. 13, pp. 400–402, 2014, doi: 10.1109/LAWP.2014.2307924.

[23]   D. Xu, S. Yin, and D. Wang, "Analysis of frequency splitting phenomena for magnetic resonance wireless power transfer systems," in *2017 Chinese Automation Congress (CAC)*, IEEE, Oct. 2017, pp. 2614–2618. doi: 10.1109/CAC.2017.8243217.

[24]   F. Nasr, M. Madani, and M. Niroomand, "Precise analysis of frequency splitting phenomenon of magnetically coupled wireless power transfer system," in *2017 IEEE Asia Pacific Microwave Conference (APMC)*, IEEE, Nov. 2017, pp. 219–224. doi: 10.1109/APMC.2017.8251418.

[25]   V. Shevchenko, O. Husev, R. Strzelecki, B. Pakhaliuk, N. Poliakov, and N. Strzelecka, "Compensation topologies in IPT systems: standards, requirements, classification, analysis, comparison and application," *IEEE Access*, vol. 7, pp. 120559–120580, 2019, doi: 10.1109/ACCESS.2019.2937891.

[26]   V. Jiwariyavej, T. Imura, and Y. Hori, "Coupling coefficients estimation of wireless power transfer system via magnetic resonance coupling using information from either side of the system," *IEEE Journal of Emerging and Selected Topics in Power Electronics*, vol. 3, no. 1, pp. 191–200, Mar. 2015, doi: 10.1109/JESTPE.2014.2332056.

[27]   T. Nakamura, T. Hirata, E. Setiawan, and I. Hodaka, "A practical method for estimating mutual inductance in wireless power transmission system," *International Journal of Circuits, Systems and Signal Processing*, vol. 16, pp. 1027–1034, Jun. 2022, doi: 10.46300/9106.2022.16.125.

[28]   Raspberry Pi Pico Datasheet, "Raspberry Pi Pico datasheet an RP2040-based microcontroller board," Raspberry Pi Ltd (formerly Raspberry Pi (Trading) Ltd.), 2023. Accessed: Jan 25, 2024 [Online]. Available: https://datasheets.raspberrypi.com/pico/pico-datasheet.pdf

[29]   Texas Instruments, "INA219 zero-drift, bidirectional current/power monitor with I2C interface," INA219, 2015. Accessed: Jan 25, 2024 [Online]. Available: https://www.ti.com/lit/ds/symlink/ina219.pdf

[30]   S. R. Akbar and I. Hodaka, "A fast spotting strategy of optimal frequency in wireless power transfer," *International Journal of Electrical and Electronic Engineering & Telecommunications*, pp. 242–246, 2020, doi: 10.18178/ijeetc.9.4.242-246.

BIOGRAPHIES OF AUTHORS

Sabriansyah Rizqika Akbar 🆔 📇 SC 🔗 is faculty member of the Faculty of Computer Science at Universitas Brawijaya since 2011. After completing a bachelor's degree in electrical engineering from Universitas Brawijaya in 2005, Sabriansyah earned a master's degree in electrical engineering from Gadjah Mada University in 2011. In that same year, he joined his alma mater as a computer engineering lecturer, now part of the Faculty of Computer Science at Universitas Brawijaya. In 2021, Sabriansyah completed his Ph.D. studies at the University of Miyazaki in the Department of Material and Informatics. He can be contacted at email: sabrian@ub.ac.id or sabrian.akbar@gmail.com.

Eko Setiawan 🆔 📇 SC 🔗 born in Kediri, went through elementary to high school education in Surabaya, pursued a bachelor's degree in electrical engineering at Universitas Brawijaya, and a master's and Ph.D. degree in electrical engineering at both Universitas Brawijaya and Miyazaki University, Japan. He can be contacted at email: ekosetiawan@ub.ac.id.

Achmad Basuki 🆔 📇 SC 🔗 is one of the senior lecturers at the Faculty of Computer Science and has been a part of Universitas Brawijaya since 2003. He holds a bachelor's degree (S1) in electrical engineering from the Department of Electrical Engineering, Universitas Brawijaya in 2000. Starting in 2006, he pursued his master's (S2) and doctoral (S3) studies in the field of cyber informatics at Keio University, Japan, completing his studies in 2012. He can be contacted at email: abazh@ub.ac.id.